Production of hydrogen as value added product from the photovoltaic thermal system operated with graphene nanoparticles: An experimental study

Production of hydrogen as value added product from the photovoltaic thermal system operated with graphene nanoparticles: An experimental study

M.Sangeetha[a], Beata Gavurova[b], Manigandan Sekar[a], Mysoon M Al-Ansari[c], Latifah A Al-Humaid[c], Quynh Hoang Le[d,e], Rajasree Shanmuganathan[d,e'*], G.K. Jhanani[f]

[a] *Department of Aeronautical Engineering, Sathyabama Institute of Science and Technology, Chennai, India*

[b] *Tomas Bata Univesity in Zlín, Faculty of Management and Economics (Mostní 5139, Zlín, 760 01, Czech Republic)*

[c] *Department of Botany and Microbiology, College of Science, King Saud University, Riyadh 11451, Saudi Arabia*

[d] *School of Medicine and Pharmacy, Duy Tan University, Da Nang, Vietnam*

[e] *Institute of Research and Development, Duy Tan University, Da Nang, Vietnam*

[f] *Center for Transdisciplinary Research (CFTR), Department of Pharmacology, Saveetha Dental College, Saveetha Institute of Medical and Technical Sciences, Saveetha University, Chennai, India*

* *Corresponding author. E-mail addresses: manisek87@gmail.com (M. Sekar), shanmuganathanrajasree@duytan.edu.vn (R. Shanmuganathan).*

ABSTRACT

Hydrogen is a growing alternative for fossil fuels that may be used to combat the energy shortfall that exists in a variety of industries, most notably the transportation and power generation industries. In this research work, the utilization of solar energy for the generation of electricity and production of hydrogen are thoroughly covered. A hybrid photovoltaic thermal system (PVT) has been used to generate the hydrogen via electrolysis process. To enhance the thermal efficiency of the PVT, graphene oxide nanofluids have been utilized. Graphene oxide nanofluids dispersed at the mass flow rates, such as 0.8 g/s, 1.0 g/s, and 1.2 g/s using sonication technique. A series of tests conducted between 9.00 A.M. to 4.00 P.M. to determine the parameters such as cell temperature, electrical efficiency, thermal efficiency and hydrogen mass flow rate. The procured results of the PVT carried out with the utilization of air and water as coolants were compared with PVT with nanofluids. From the findings it is evident that the performance of the system was significantly enhanced by the utilization of nanofluids at the optimized concentration compared to conventional water and air. With regard to the nanofluids mass flow rate, concentration of 1.2 g/s reported higher electrical (8.6%) and thermal efficiency (33.3%) compared to water. Added to above, there is a profound increase in the mass flow rate of hydrogen that has been observed at 1.2 g/s.

Keywords: Photovoltaic thermal system Nanofluids Renewable energy Nanoparticles

1. Introduction

Hydrogen is a common element in the natural world and may be broken down into its most fundamental state, which consists of only a single electron and a single proton. After many hours devoted to studying and developing new technologies, experts have arrived at the conclusion that hydrogen has the potential to replace traditional fuels **[1-3]**. The rising levels of carbon emissions, particularly those caused by the combustion of fossil fuels, have brought widespread attention to a number of related but distinct concepts, such as ecological footprint and carbon footprint. Hydrogen fuel is an emission-free fuel that may contribute to carbon neutrality, implementation of them in the energy market is an important step toward achieving the long-term aim of lowering the dangers associated with climate change **[4,5]**. Hydrogen is the most common and fundamental of the elements that may be found in the natural resources. In addition to being an alkali metal, it is known to possess characteristics of halogens. In addition to this, the capability of hydrogen to generate a significant amount of heat when it is burned in the presence of oxygen has led some people to consider it a viable alternative to traditional fossil fuel **[6,7]**. The fuel that is formed as a result of the combustion of hydrogen in the presence of oxygen is a fuel that produces no emissions and may effectively contribute to the upkeep of carbon neutrality.

Nomenclature

P_0	Electrical output power (W)
V	Voltage across the load (V)
I	Photo-current of the solar cell (A)
A	Panel area (m2)
$\dot{m}$	mass flow rate (kg/s)
Te	exit fluid temperature (° C)
T_i	inlet fluid temperature (°C)
P	is the density (g/s)

Subscript

P	np and f represents nanoparticle, fluid and nanofluid respectively.
Ø	is the volumetric fraction.
P_E	Electrical power
P*c*	Cooled power (W)
P_i	Reference electrical power (W)
P_m	Maximum power output (W)
P_{SIN}	Power due to solar radiation (W)

Not only can the hydrogen fuel cell create sufficient amounts of energy in comparison to other fuels, but it is also recognized for being the source of the fewest pollutants released into the atmosphere. Oxygen and hydrogen together are known to produce water as a by-product during the generation of power when they are combined **[7-10]**. In addition, it is typical that hydrogen fuel cells go through the process of electrolysis, in which the electrically charged particles move from one electrode to another **[11,12]**. Recently, the use of nanofluids in the energy sector has been increasing rapidly. Nanoparticles may be divided into three categories: those based on metal, those based on carbon, and nanocomposites. The nanoparticles that are based on metals may be further subdivided into two groups: metals and metal oxides, which are chemical compounds that consist of the elements metal and oxygen **[13,14]**. Carbon nanotubes (CNT) with a cylindrical nanostructure, and graphene (GO), which is carbon in the form of a twodimensional allotrope, are two of the several forms of carbon-based nanoparticles that may be distinguished from one another **[15,16]**. Nanocomposites, which stand out among the other types of nanoparticles due to their unique composition. This class includes two distinct varieties of particles that each has sizes of less than 100 nm. The ceramic matrix, the metal matrix, and the polymer matrix are the possible categories for describing these nanocomposites **[17,18]**. Nanoparticles have a number of advantageous properties, including increasing the thermal conductivity of the working fluid, which in turn improves the heat transfer coefficient of the working fluid; By increasing the fluid's density and specific heat product, we make it possible for the fluid to transport significant amounts of thermal energy **[19]**. Increasing the rate at which heat is transferred from the fluid to the receiver, enhances the efficiency of the PV system in terms of both its thermal and electrical output; Bringing the temperature of the absorber down and, as a result, safeguarding the material. There are two ways to create nanofluid, the first of which is a single process, and the second of which involves two steps. During this stage of the process, both the dispersion and the synthesis of nanoparticles take place simultaneously **[20,21]**. This procedure can be executed using either physical or chemical means, depending on the situation. For the synthesis of nanoparticles using the physical technique, an ultrasonic-aided submerged arc system is utilized. The chemical technique requires the addition of a reducing agent to the combination of nanoparticles and base fluid, which is then followed by stirring and heating. The nanoparticles are created during the first step of the Two-Step Method, which is followed by the mixing of the nanoparticles and the base fluid using high shear or ultrasonic **[22]**.

When a mixture is subjected to direct sonication, it indicates that the ultrasonic probe or horn is coming into direct touch with the mixture. During this stage of the procedure, the nanoparticles and the base fluid are both measured out by weight before being poured into a container together. After giving the combination a one-minute stir with a very thin metal rod, it should be subjected to direct ultrasonication for a period of 30 to 45 min. However, if the nanofluid is created by employing the ultrasonic bath or pulsed ultrasonic, then this method will be classified as indirect sonication since the ultrasonic waves will be introduced in a more indirect manner. In this instance, the nanoparticles and the host fluid are stored within a vessel that is submerged in a bath **[23]**. The vessel is kept at room temperature. Ultrasonic pulsations can be transmitted in this bath to its porous surface. This approach is not recommended for use with nanofluids that have a high viscosity base. In contrast to the ultrasonication process, the high-pressure homogenizer is often regarded as the most efficient way the creation of nanofluid. Nevertheless, this method has a few drawbacks, including a massive size and weight, a significant price tag, and a restricted processing capacity all at once. Another method of mixing is the use of a mechanical stirrer, also called an overhead stirrer, which is capable of mixing amounts as big as 25 L. In contrast to previous treatment approaches, this one does not prevent the aggregation of particles as effectively as the others do. In addition to the methods that have been discussed so far, a shaker, also known as dispersion, is an option for the creation of nanofluids in

natural settings. In addition to this, the process of forming nanofluids by combining nanoparticles and refrigerants using this method is quite effective **[27-29]**. This concoction is referred to as nano refrigerant. Additionally, it can be beneficial for gases and fluids operating at low temperatures. Because of the wide variety of uses they have, graphene oxide nanoparticles, also known as GONPs, have garnered a lot of attention. Some of the notable studies predicted the effectiveness of the nanofluids in the PVT. Hybrid systems are used to enhance the electrical output by decreasing the cell temperature. From the above literature study, it is evident that the use of the nanoparticle enhances the production of electrical output by cooling the PV cell temperature which indeed produces hydrogen.

2. Methodology

2.1. Nanofluid preparation

Because of the wide variety of uses they have, graphene oxide nanoparticles, also known as GONPs, have gathered a lot of attention. Ultrasonication was the method that was utilized during the production of GONF (Graphene Oxide Nano Fluid). There are several outcomes that may be achieved through the utilization of ultrasonic nanoparticle dispersion. The most straightforward strategy involves dispersing materials in liquids in order to break up agglomerates of particle clusters. The use of ultrasound during the synthesis of particles or the precipitation of such particles is still another method. In addition, ultrasonic cavitation facilitates an improvement in the material transfer that takes place at particle surfaces. Because of this effect, the surface functionalization of materials that have a high specific surface area can be improved. GONP were subsequently distributed in water as a result of the ultrasonication process. Prior to the ultrasonication process, the nanoparticles were exposed to treatment on the heating surface for at least an 1 h at a temperature of 200 ° C to eliminate any trace of moisture that may have been present in the nanoparticles **[24].** After the application of the pre-treatment, which consisted of heating the particles, the nanoparticles were put through 420 min of progressive and steady sonication at a frequency of 25 kHz. For the purpose of dispersing the nanoparticles and incorporating them into the PV/T, the ultrasonication approach was used. Due to the fine dispersion, the colour of the combination should be changed after the sonication process **[30-32]**. The correct mixing of the ingredients may be achieved by continuing the ultrasonication process without a break for at least seven hours. Table 1 shows the properties of the nanofluids.

2.2. Experimental setup

In order to carry out this research, an experimental setup consisting of two solar collectors was established. One of the solar collectors consisted of solely a photovoltaic (PV) module, while the other consisted of a PV module in conjunction with a thermal collector. The ’k’ type thermocouple, the flow meter, the storage tank with a capacity of 15 L, the pump, the compressor, the flow control valve, and the heat exchanger unit were the instruments that were utilized. Fig. 1 shows the experimental layout. The testing apparatus was made up of a polycrystalline PV module with a power output of 60 W and a heat collector constructed out of a copper tube with an outer diameter of 13.5 mm and an inner diameter of 11.5 mm. A copperplate that is 6 mm thick is used to make the connection between the back of the PV module and the thermal collector. A flow control valve was used to adjust the flow rate of the fluid, and a flow meter was used to determine how much fluid is being moved through the system.

Table 1 Properties of nanofluid.

nanoparticle	GPO
Diameter	23–27 nm
Surface area	495 m^2/g
Purity	99 %
Thermal conductivity	3000 W/mK

A heat transfer unit was used to bring the temperature of the water down so that it may be reused in the system. This allows the water to be recycled. A thermocouple was utilized in order to obtain readings regarding the temperature of the panel's surface as well as the fluid on both the input and output sides. Through the utilization of a data collection system, the real readings were acquired, recorded, and preserved in the central processing unit. (DAQ) **[33,34]. Table 2** shows the specifications of experimental test rig. The Hoffman electroplating device was put to use in this investigation so that hydrogen gas can be produced. In order to determine the level of purity of the hydrogen gas that was generated, a hydrogen quality tester was utilized. The tests were conducted from 9:00 A.M. to 4:00 P.M. on hourly intervals at the month of June 2022. In addition to the production of electricity, this study makes use of Hoffman' s hydrogen production system to produce hydrogen, which was then analyzed in terms of its contribution to the overall production rate of the solar-assisted hydrogen production system **[25].** The use of electrical energy allows for the separation of water into its component gases of hydrogen (H_2) and oxygen (O_2) in this system. During this process, the PVT solar collector was where the energy for the electrical generator was collected.

The following formulas were used for the calculation of electrical output, electrical efficiency and specific heat.

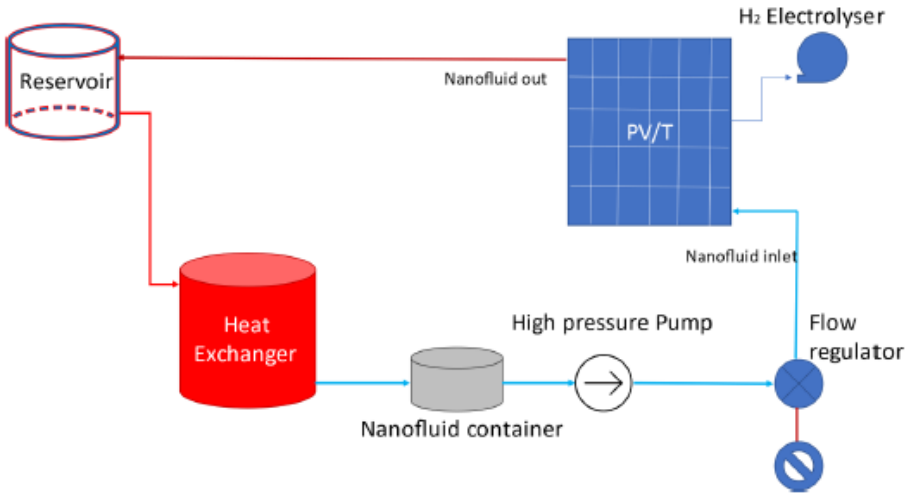

Fig. 1. Experimental layout.

The electrical output **[34]** given by

$$P_0 = (V*I)A \quad (1)$$

The maximum power **[34]** output

$$P_{maximum} = V*I \quad (2)$$

$$Q_s = h*C_{nf}\ (T_e - T_i \quad (3)$$

Where:

Specific heat od nanofluid (C_{nf}) **[35]** can be expressed as below

$$c_{nf} = \frac{\rho_p \varnothing c_{p,np} + \rho_f c_{p,j}(1-\varnothing)}{\rho_p \varnothing + \rho_f (1-\varnothing)} \quad (4)$$

Electrical power is represented by

$$\%P_E = \frac{P_c - P_i}{P_i} * 100 \quad (5)$$

The electrical effciency of the panel due to solar irradiance (η_{esr}) **[36]** can be measured by dividing with power out as follows,

$$h_{esr} = \frac{P_m}{P_{SIN}} \quad (6)$$

Table 2 Specification of PVT Instrumentation.

Number of tubes	20
Copper tube inner diameter	11.5
Outer diameter	13.5
Output power	60 W
Copperplate depth	8 mm
Thermocouple	k-Type
Thermal collector type	Copper sheet/tube
Pump	DC
Voltage	25 V
Short circuit Current	2.5 Amp
Depth of the copper plate	8 mm

3. Results and discussion

The heat transfer qualities of the resultant nanofluid are impacted not only by the thermophysical properties of the added nanoparticles but also by those of the base fluid. The precise formulation of a nanofluid has a significant impact on the varied thermal conductivity characteristics of the nanofluid. Due to the fact that the density, viscosity, and thermal conductivity of a nanofluid each play a significant influence on the features of the nanofluid's heat transfer, the initial tests focused on analyzing these qualities. In the testing, the nanofluid was tested at temperatures ranging from 30 °C to 60 °C. This temperature range corresponds to the conducting range of the system. The properties calculated for the nanofluid proportions were calculated for the reference air and water. In addition

to it, the PV Panel temperature, outlet fluid temperature, thermal efficiency, electrical efficiency, and hydrogen production rate were also measured.

3.1. Density

Fig. 2 illustrates how the density of the fluids that were sampled at different temperatures, ranging from 30 ° C to 60 °C, fluctuates. The density will increase in direct proportion to the number of nanoparticles that are added. When compared to the density of air, water has a higher specific gravity. Nanoparticles combined with water have a higher density than air. According to the findings, increasing the nanoparticle percentage led to a rise in the nanofluid density, whereas an increase in temperature led to a decrease in the density [28]. The lowest density was for air while the highest was for the higher nanoparticles rate of 1.2 g/s. The Water + 1.2 GP nanofluid had the density values at the temperatures of 30 ° C, 40 °C, 50 °C and 60 °C were 1.0063 g/s, 0.9942 g/s, 0.99 g/s and 0.9857 g/s respectively.

3.2. Viscosity

The impact of heat on the viscosity of the nanofluid, air, and water were qualitatively comparable. However, the rate at which the nanofluid's viscosity decreased with a rise in temperature is dependent on the concentration of nanoparticles in the nanofluid. It was proved that directly increasing the concentration of nanoparticles in a liquid can have an effect on the liquid's internal shear stress. According to the findings of this study, a rise in temperature reduces the adhesion forces between the molecules, which, in turn, results in lower shear stress. The relationship between viscosity and temperature is illustrated in **Fig. 3**, which can be found below. The viscosity values of air at all temperature were lower than the other used fluids. The second higher rate was for water than it was for used nanofluids. As the added nanoparticles level was increased, the viscosity of the nanofluids was also increased **[28,37]**. The 1.2 g GP added water viscosity at the temperatures of 30 °C, 40 °C, 50 °C, and 60 °C were 1.015 mPas, 0.958 mPas, 0.932 mPas, and 0.917 mPas respectively. The least viscosity was found in the air with values of 0.975 mPas, 0.924 mPas, 0.91 mPas and 0.906 mPas.

3.3. Thermal conductivity

To attain greater thermal conductivities in nanofluids in comparison to those of the base fluid is the primary objective of the research that is being done on this topic. The increase in thermal conductivity seen in **Fig. 4** is directly correlated to both an increase in temperature and an increase in the concentration of graphene nanoparticles. A higher temperature significantly accelerates the rate at which particles collide, leading to a greater accumulation of kinetic energy in the system. The same pattern that we noticed in the density of the used coolants was observed in thermal conductivity too **[37,38]**. The lowest was in the air and the highest was in the water with 1.2 g/s GP nanoparticles concentration. The thermal conductivity higher order goes in the order of air, water, water + 0.8 g/s, water + 1.0 g/s, and water + 1.2 g/s. The values of the water + 1.2 g/s were 0.673 W/mK, 0.694 W/mK, 0.71 W/ mK, and 0.723 W/mK at the temperature from 30 °C to 60 °C with 10 °C-intervals.

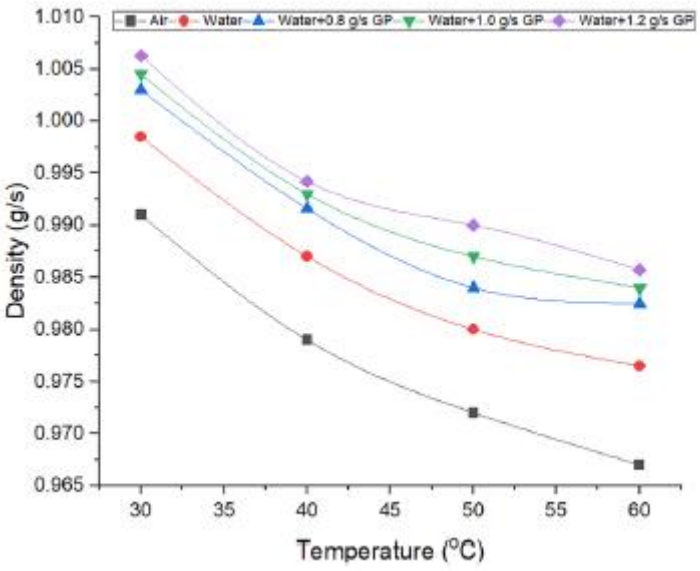

Fig. 2. Density at variable temperatures.

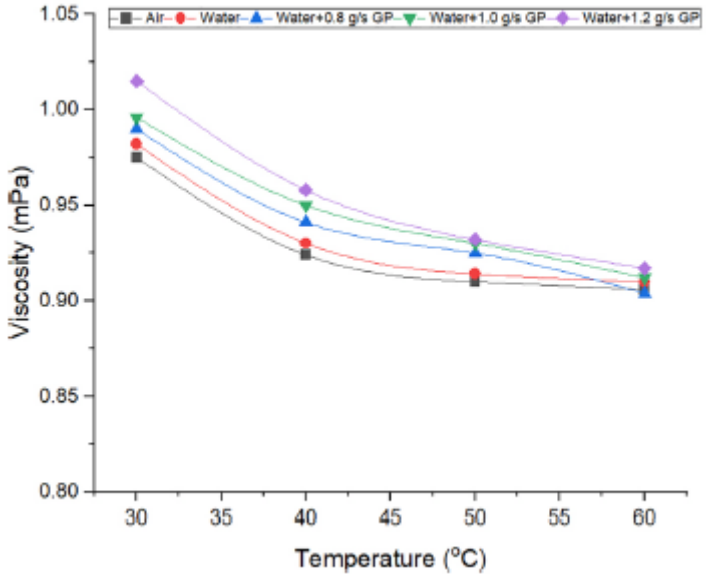

Fig. 3. Viscosity at variable temperatures.

3.4. Cell temperature

Fig. 5 shows the cell temperature variations at various test conditions. The tests were carried out at regular intervals of one hour from 9:00 A.M. to 4:00 P.M. The cell temperature is the same as the temperature of the photovoltaic panel, and it indicates how much of its irradiation is provided by the sun. Regardless of the results of the samples, it is a well-known truth that the temperature is lower at eight in the morning, that it steadily increases until 12 P.M., and that it then drops again in the evening. It was observed that there was a corresponding shift in the panel's temperature. The temperature of the cell was found to be at its lowest at 8.00 A.M., and at its greatest at middle of the day **[35]**. The

respective temperature variation of air from 9:00 A.M. to 4:00 P.M. were 60 °C, 62.5 °C, 67.5 °C, 72 °C, 68 °C, 66.4 °C, 62 °C, and 61.1 °C. As the day time goes, the cell temperature reduces due to the radiation reduction from the sun and also as the amount of given nanofluid is increased, the panel cell temperature is reduced due to the dispersed nanoparticles that absorb the cell temperature. the panel temperature is effectively reduced by the use of water + graphene nanoparticles **[33]**. Through convection and conduction mode the heat is transferred from the PV panel cell.

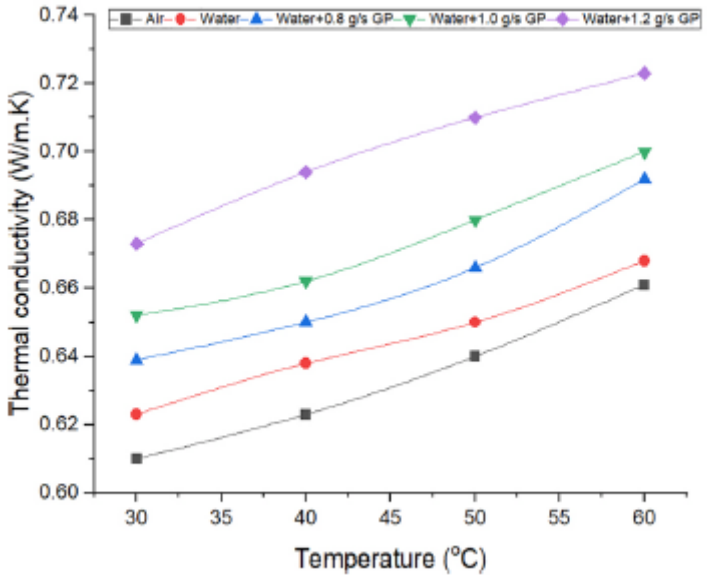

Fig. 4. Thermal conductivity at variable temperatures.

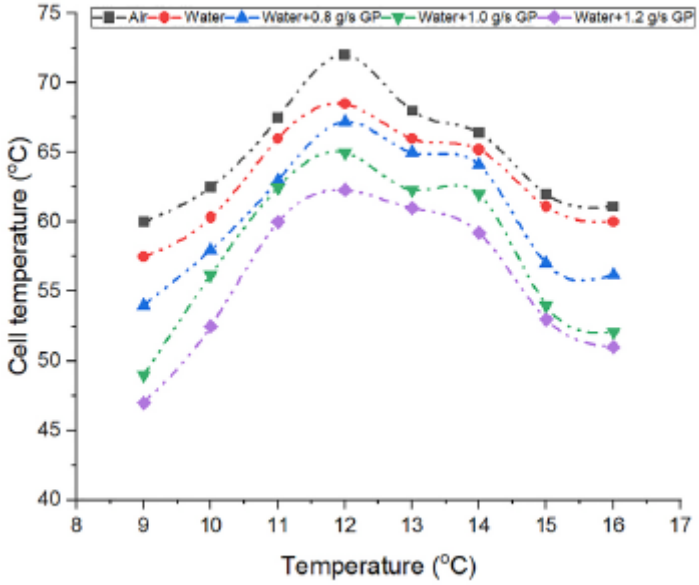

Fig. 5. Cell temperature at variable temperatures.

3.5. Fluid outlet temperature

Calculating the thermal conductivity of various substances, such as air, water, and utilized nanoparticles enable one to determine the efficacy of those substances. The sample will have a better capacity to absorb heat from the photovoltaic cell in proportion to the thermal conductivity it possesses. If the temperature of the cell is lower, then the amount of outflow fluid will have a greater temperature**. Fig. 6** shows the variance in the fluid outlet temperature with respect to time of the day. The highest fluid outlet temperature was noted at 12:00 P.M. since the global temperature is highest at that time and the heat absorption by the samples used to collect the greater heat in it and thus the outlet temperature is increased **[34,41].** The increased mass flow rate of the nanofluids increased the amount of heat transfer. The water with the 1.2 g/s graphene nanofluid showed the highest transfer rate with the peak fluid outlet temperature. The highest temperature of the fluid used air, water, water + 0.8 g/s, water + 1.0 g/s, and water + 1.2 g/s were 34.3 ° C, 37 °C, 38.2 °C, 39.5 °C and 42 °C respectively.

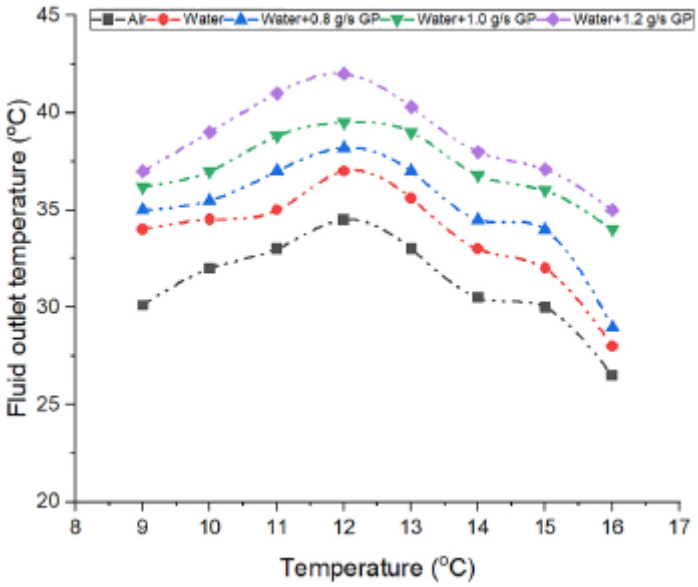

Fig. 6. Fluid outlet temperature for various samples.

3.6. Thermal efficiency

The quantity of thermal efficiency that the utilized sample possessed at various times of the day is shown in a straightforward and concise manner in **Fig. 7**a. The thermal efficiency of the fluid that is being utilized is dependent not only on the thermal conductivity of the fluid but also on the temperature at which the fluid is being let out. Because of the increased number of nanoparticles that come into touch with the PV panel surface when the mass flow rate is high, there are more points of contact between the fluid and the surface of the panel. This causes an increase in the temperature at which the fluid exits the panel. The fluid outlet temperature and the thermal conductivity of the samples both follow the same pattern, which is also followed by the thermal efficiency of the samples **[26]**. According to the same pattern, the most effective time for all of the samples was determined to be 12.00 P.M. in the afternoon. It was found that water combined with 1.2 g/s nanoparticles had the highest efficiency. When compared to air and water, the water with nanoparticles added had a higher

thermal efficiency **[36,40]**, and this was observed even at a mass flow rate of 0.8 g/s. The lowest thermal efficiency was noticed in the air sample with values of 18.5 %, 22.5 %, 24 %, 27 %, 25.2 %, 23 %, 22.2 %, and 21.6 % respectively from 9:00 A. M to 4:00 P.M. The water + 1.2 g/s sample values were 25 %, 28.2 %, 31 %, 33.4 %, 32.5 %, 30 %, 28.8 % and 28 % respectively.

3.7. Electrical efficiency

The fluctuation in the electrical efficiency provided by the samples that were obtained throughout the day is depicted in a clear and concise manner in **Fig. 7b**. The thermal conductivity of the fluid, the temperature of the fluid outflow, and the temperature of the PV wall all have a role in determining the electrical efficiency of the fluid. The fluid's electrical efficiency improves in direct proportion to the decrease in wall temperature **[44]**. Because of how well the fluid absorbs heat from the PV wall, the rate at which heat is transferred is precisely proportional to the temperature at which the fluid exits the system. The gradual variance in temperature was observed in all kinds of samples used. Thermal efficiency is linked to electrical efficiency so similar results are only obtained in the models used. With respect to global solar radiation, the temperature and thus the electrical efficiency were changed **[34,42]**. From morning 9:00 A.M. to 12:00 P.M., the electrical efficiency was increased and reached its peak value at 12:00 P.M., then it started to reduce. The highest and lowest electrical efficiency obtained by water + 0.0012 g/s graphene nanofluid and air were 2.9 %, 5.2 %, 6.91 %, 8.6 %, 7.4 %, 6.9 %, 6.52 %, 6.2 % and 2.3 %, 4.4 %, 6.3 %, 7.32 %, 6.6 %, 5.9 %, 5.5 %, 5.3 % respectively.

3.8. Hydrogen flow rate

Electrolysis is the process that is utilized to create hydrogen by the separation of water into its component oxygen and hydrogen atoms. In this instance, the photovoltaic panel was utilized to generate energy, and the electricity that was generated was put to use in the generation of hydrogen via PEM electrolyser. **Fig. 8** depicts the production rate of hydrogen based on the different global radiation.

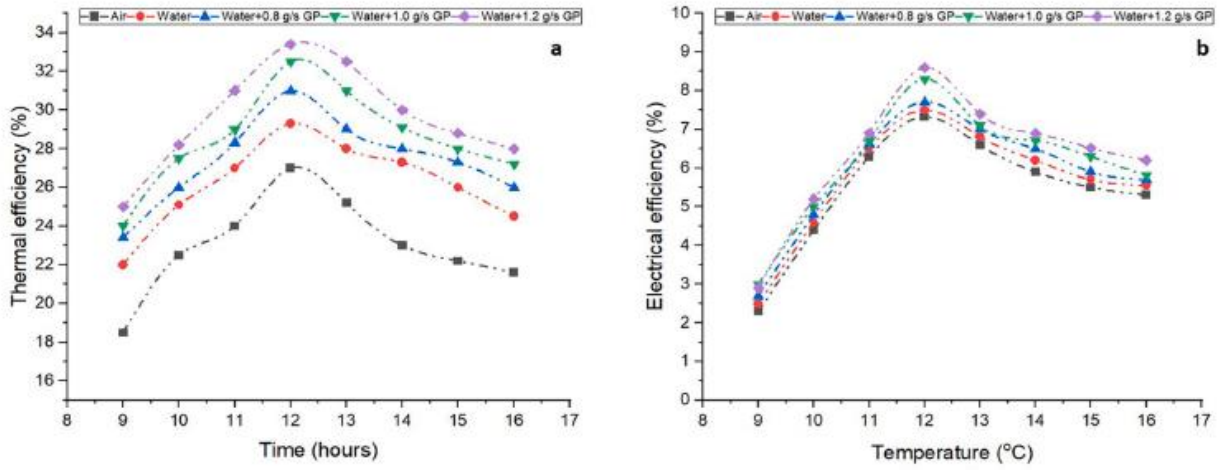

Fig. 7. (a) Thermal efficiency for various conditions. (b) Electrical efficiency for various conditions.

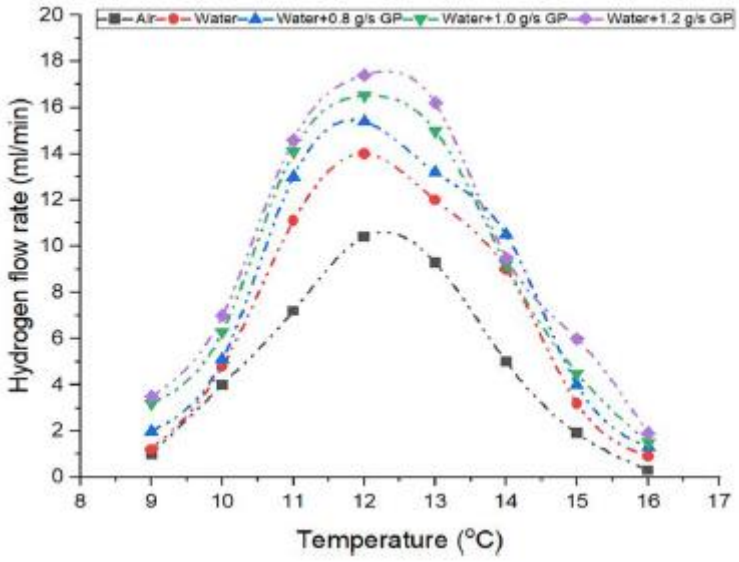

Fig. 8. Hydrogen flow rate for various conditions.

The pace of hydrogen synthesis picked up alongside the rise in the amount of power generated. The variation in the amount of power that was obtained was in relation to the temperature change. Similarly, the rate of hydrogen generationunderwent some adjustments as well **[39]**. The maximum rate of hydrogen generation was observed around twelve o'clock in the afternoon, while the lowest rate was measured at four o'clock. The water with a higher mass flow rate of graphene nanoparticles at 1.2 g/s produced greater hydrogen than other samples used at 12:00 P.M. with the value of 17.4 ml/min **[43]**. The lowest production of hydrogen was seen in the air sample throughout the day.

4. Conclusion

The experimental research was conducted in a PVT solar system, and the power generated was put to use in an electrolysis process to generate hydrogen. In addition, a variety of samples were utilized in an effort to improve the efficiency of the PVT solar system. Air, water, and water with 0.8 g/s, 1.0 g/s, and 1.2 g/s added were the samples that were utilized. It was determined how effective the fluids that were employed were. During the day, the recordings were made between the hours of 9:00 A.M. and 4:00 P.M. At first, the characteristics of samples that were going to be utilized were examined, such as their density, viscosity, and thermal conductivity. After that, the temperature of the cell, the temperature of the fluid outlet, the electrical efficiency, the thermal efficiency, and the rate of hydrogen generation were determined. The findings make it quite obvious that the outcomes mostly differed depending on the time of day, which can be understood and concluded from the findings themselves. The performance of the system was significantly improved by the application of nanofluids. Specifically, the mass flow rate of graphene nanofluids that are employed will determine the level of improvement in performance that may be expected. When compared to air and water, the water that had 1.2 g/s nanoparticles added to it showed the highest electrical efficiency, thermal efficiency, fluid outlet temperature, and hydrogen production rate with the values of 8.6 %, 33.4 %, 42 ° C, and 17.4 ml/m in at 12 P.M. This is due to the fact that at that time only the available solar radiation

is at its highest level, making it possible for the system to effectively convert heat. From the above findings it is clear the use of the nanofluids can be the potential option to increase the thermal efficiency of the system and the opportunity to produce hydrogen via the electrolysis process was highly desirable.

References

[1] Younas M, Shafique S, Hafeez A, Javed F, Rehman F. An overview of hydrogen production: current status, potential, and challenges. Fuel 2022 May;15(316): 123317.

[2] Sekar M, Kumar TP, Kumar MS, Vanícková R, Marousek J. Techno-economic review on short-term anthropogenic emissions of air pollutants and particulate matter. Fuel 2021 Dec;1(305):121544.

[3] Tian Z, Wang Y, Zhen X, Liu D. Numerical comparative analysis on performance and emission characteristics of methanol/hydrogen, ethanol/hydrogen and butanol/hydrogen blends fuels under lean burn conditions in SI engine. Fuel 2022 Apr;1(313):123012.

[4] Sarkodie SA. Environmental performance, biocapacity, carbon & ecological footprint of nations: Drivers, trends and mitigation options. Sci Total Environ 2021 Jan;10(751):141912.

[5] Nair M, Arvin MB, Pradhan RP, Bahmani S. Is higher economic growth possible through better institutional quality and a lower carbon footprint? Evidence from developing countries. Renewable Energy 2021 Apr;1(167):132-45.

[6] Gunasekar P, Manigandan S, TR PK. Hydrogen as the futuristic fuel for the aviation and aerospace industry-review. Aircraft Engineering and Aerospace Technology. 2020 Dec 30.

[7] Marousek J. Nanoparticles can change (bio) hydrogen competitiveness. Fuel 2022 Nov;15(328):125318.

[8] Felseghi RA, Carcadea E, Raboaca MS, Trufin CN, Filote C. Hydrogen fuel cell technology for the sustainable future of stationary applications. Energies 2019 Dec 3;12(23):4593.

[9] Yue M, Lambert H, Pahon E, Roche R, Jemei S, Hissel D. Hydrogen energy systems: A critical review of technologies, applications, trends and challenges. Renew Sustain Energy Rev 2021 Aug;1(146):111180.

[10] Dawood F, Anda M, Shafiullah GM. Hydrogen production for energy: An overview. Int J Hydrogen Energy 2020 Feb 7;45(7):3847-69.

[11] Wang S, Lu A, Zhong CJ. Hydrogen production from water electrolysis: Role of catalysts. Nano Convergence 2021 Dec;8(1):1-23.

[12] Anwar S, Khan F, Zhang Y, Djire A. Recent development in electrocatalysts for hydrogen production through water electrolysis. Int J Hydrogen Energy 2021 Sep 13;46(63):32284-317.

[13] Shao D, Al Obaid S, Alharbi SA, Marousek J, Sekar M, Gunasekar P, et al. Prediction of the fuel spray characteristics in the combustion chamber with methane and TiO2 nanoparticles via numerical modelling. Fuel 2022 Oct;15(326): 124820.

[14] Ge S, Brindhadevi K, Xia C, Khalifa AS, Elfasakhany A, Unpaprom Y, et al. Enhancement of the combustion, performance and emission characteristics of spirulina microalgae biodiesel blends using nanoparticles. Fuel 2022 Jan;15(308): 121822.

[15] Zhang X, Yang R, Anburajan P, Van Le Q, Alsehli M, Xia C, et al. Assessment of hydrogen and nanoparticles blended biodiesel on the diesel engine performance and emission characteristics. Fuel 2022 Jan;1(307):121780.

[16] Vinayan BP, Sethupathi K, Ramaprabhu S. Facile synthesis of triangular shaped palladium nanoparticles decorated nitrogen doped graphene and their catalytic study for renewable energy applications. Int J Hydrogen Energy 2013 Feb 19;38 (5):2240-50.

[17] Ansu AK, Sharma RK, Hagos FY, Tripathi D, Tyagi VV. Improved thermal energy storage behavior of polyethylene glycol-based NEOPCM containing aluminum oxide nanoparticles for solar thermal applications. J Therm Anal Calorim 2021 Feb;143(3):1881-92.

[18] Ma T, Guo Z, Lin M, Wang Q. Recent trends on nanofluid heat transfer machine learning research applied to renewable energy. Renew Sustain Energy Rev 2021 Mar;1(138):110494.

[19] Okonkwo EC, Wole-Osho I, Almanassra IW, Abdullatif YM, Al-Ansari T. An updated review of nanofluids in various heat transfer devices. J Therm Anal Calorim 2021 Sep;145(6):2817-72.

[20] Hanbazazah AS, Ali A, Alsaady M, Yan Y, Murshid G, Khoo KS, et al. Optimization and experimental analysis of sustainable solar collector efficiency under the influence of magnetic nanofluids. Applied Nanoscience 2022 Jul;12:1-2.

[21] Pavía M, Alajami K, Estellé P, Desforges A, Vigolo B. A critical review on thermal conductivity enhancement of graphene-based nanofluids. Adv Colloid Interface Sci 2021 Aug;1(294):102452.

[22] Smaisim GF, Abdulhadi AM, Uktamov KF, Alsultany FH, Izzat SE, Ansari MJ, et al. Nanofluids: properties and applications. J Sol-Gel Sci Technol 2022 Jul;2:1-35.

[23] Said Z, Sundar LS, Tiwari AK, Ali HM, Sheikholeslami M, Bellos E, et al. Recent advances on the fundamental physical phenomena behind stability, dynamic motion, thermophysical properties, heat transport, applications, and challenges of nanofluids. Phys Rep 2021 Jul 19.

[24] Azimy H, Meghdadi Isfahani AH, Farahnakian M. Investigation of the effect of ultrasonic waves on heat transfer and nanofluid stability of MWCNTs in sono heat exchanger: an experimental study. Heat Mass Transf 2022 Mar;58(3):467-79.

[25] Gul M, Akyuz E. Hydrogen generation from a small-scale solar photovoltaic thermal (PV/T) electrolyzer system: Numerical model and experimental verification. Energies 2020 Jun 10;13(11):2997.

[26] Choi HU, Choi KH. Performance evaluation of PV/T air collector having a singlepass double-flow air channel and non-uniform cross-section transverse rib. Energies 2020 May 2;13(9):2203.

[27] Sardarabadi M, Passandideh-Fard M, Heris SZ. Experimental investigation of the effects of silica/water nanofluid on PV/T (photovoltaic thermal units). Energy 2014 Mar;1(66):264-72.

[28] Al-Waeli AH, Sopian K, Chaichan MT, Kazem HA, Hasan HA, Al-Shamani AN. An experimental investigation of SiC nanofluid as a base-fluid for a photovoltaic thermal PV/T system. Energy Convers Manage 2017 Jun;15(142):547-58.

[29] Shahsavar A, Alwaeli AH, Azimi N, Rostami S, Sopian K, Arici M, et al. Exergy studies in water-based and nanofluid-based photovoltaic/thermal collectors: Status and prospects. Renew Sustain Energy Rev 2022 Oct;1(168):112740.

[30] Fu Y, Mei T, Wang G, Guo A, Dai G, Wang S, et al. Investigation on enhancing effects of Au nanoparticles on solar steam generation in graphene oxide nanofluids. Appl Therm Eng 2017 Mar;5(114):961-8.

[31] Chaichan MT, Kamel SH, Al-Ajeely AN. Thermal conductivity enhancement by using nano-material in phase change material for latent heat thermal energy storage systems. Saussurea 2015;5(6):48-55.

[32] Abdelrazik AS, Tan KH, Aslfattahi N, Saidur R, Al-Sulaiman FA. Optical properties and stability of water-based nanofluids mixed with reduced graphene oxide decorated with silver and energy performance investigation in hybrid photovoltaic/thermal solar systems. Int J Energy Res 2020 Nov;44(14):11487-508.

[33] Manigandan S, Kumar V. Comparative study to use nanofluid ZnO and CuO with phase change material in photovoltaic thermal system. Int J Energy Res 2019 Apr; 43(5):1882-91.

[34] Sangeetha M, Manigandan S, Chaichan MT, Kumar V. Progress of MWCNT, Al2O3, and CuO with water in enhancing the photovoltaic thermal system. Int J Energy Res 2020 Feb;44(2):821-32.

[35] Abdallah SR, Saidani-Scott H, Abdellatif OE. Performance analysis for hybrid PV/T system using low concentration MWCNT (water-based) nanofluid. Sol Energy 2019 Mar;15(181):108-15.

[36] Al-Waeli AH, Chaichan MT, Kazem HA, Sopian K. Comparative study to use nano-(Al2O3, CuO, and SiC) with water to enhance photovoltaic thermal PV/T collectors. Energy Convers Manage 2017 Sep;15(148):963-73.

[37] Fedele L, Colla L, Bobbo S. Viscosity and thermal conductivity measurements of water-based nanofluids containing titanium oxide nanoparticles. Int J Refrig 2012 Aug 1;35(5):1359-66.

[38] Azmi WH, Sharma KV, Mamat R, Najafi G, Mohamad MS. The enhancement of effective thermal conductivity and effective dynamic viscosity of nanofluids-A review. Renew Sustain Energy Rev 2016 Jan;1(53):1046-58.

[39] Anderson A, Brindhadevi K, Salmen SH, Alahmadi TA, Marouskova A, Sangeetha M, et al. Effects of nanofluids on the photovoltaic thermal system for hydrogen production via electrolysis process. Int J Hydrogen Energy 2022 Jan 31.

[40] Sangeetha M, Manigandan S, Ashok B, Brindhadevi K, Pugazhendhi A. Experimental investigation of nanofluid based photovoltaic thermal (PV/T) system for superior electrical efficiency and hydrogen production. Fuel 2021 Feb;15(286): 119422.

[41] Al-Waeli AH, Kazem HA, Chaichan MT, Sopian K. A review of photovoltaic thermal systems: Achievements and applications. Int J Energy Res 2021 Feb;45(2): 1269-308.

[42] Al-Waeli AH, Sopian K, Kazem HA, Chaichan MT. Evaluation of the electrical performance of a photovoltaic thermal system using nano-enhanced paraffin and nanofluids. Case Studies in Thermal Engineering 2020 Oct;1(21):100678.

[43] Senthilraja S, Gangadevi R, Marimuthu R, Baskaran M. Performance evaluation of water and air based PVT solar collector for hydrogen production application. Int J Hydrogen Energy 2020 Mar 6;45(13):7498-507.

[44] Al-Waeli AH, Chaichan MT, Kazem HA, Sopian K. Evaluation and analysis of nanofluid and surfactant impact on photovoltaic-thermal systems. Case Stud Therm Eng 2019 Mar;1(13):100392.